KSME International Journal, Vol. 16 No. 11, pp. 1457~1469, 2002

Experimental Study on Axial Stratification Process and Its Effects (I)
— Stratification in Engine —

In-Yong Ohm*, Chan Jun Park
Department. of Mechanical Engineering, Seoul National University of Technology, Seoul 139-743, Korea

This paper is the first of several companion papers, which investigate axial stratification process and its effects in an SI engine. The axial stratification is very sophisticate phenomenon, which results from combination of fuel injection, port and in-cylinder flow and mixing. Because of the inherent unsteady condition in the reciprocating engine, it is impossible to understand the mechanism through the analytical method. In this paper, the ports were characterized by swirl and tumble number in steady flow bench test. After this, lean misfire limit of the engines, which had different port characteristic, were investigated as a function of swirl ratio and injection timing for confirming the existence of stratification. In addition, gas fuel was used for verifying whether this phenomenon depends on bulk air motion of cylinder or on evaporation of fuel. High-speed gas sampling and analysis was also performed to estimate stratification charging effect. The results show that the AFR at the spark plug and LML are very closely related and the AFR is the results of bulk air motion.

Key Words : Stratification, Steady Flow Bench, Swirl Ratio, Injection Timing, Lean Misfire Limit

Nomenclature

A : Number of intake valve
B : Bore
CI : Center injection
HPI : Helical port injection
BPO : Both ports open
FPO : Front port open
RPO : Rear port open
C_f : Flow coefficient
C_M : Concentration of methanol
C_S : Swirl coefficient
C_T : Tumble coefficient
D : Inner seat diameter of intake port
LML : Lean misfire limit
M : Moment of momentum flux
N : Engine speed
N_{vl} : Non dimensional valve lift, L/D
RS : Ricardo swirl number
S : Stroke
$\dot{m}$: Mass flow rate
v_a : Axial velocity
v_t : Tangential velocity
v_0 : Characteristic velocity derived from the pressure drop across the valve
λ : Non dimensional air-fuel ratio, divided by stoichiometric
ρ : Air density
θ : Crank angle
ω_s : Angular velocity of a solid body rotating flow

* Corresponding Author,
E-mail : iyohm@snut.ac.kr
TEL : +82-2-970-6311; **FAX** : +82-2-949-1458
Dept. of Mechanical Engineering, Seoul National University of Technology 172, Gongreung 2-Dong, Nowon-Gu Seoul 139-743, Korea. (Manuscript **Received** September 22, 2001; **Revised** August 27, 2002)

1. Introduction

The purpose of this study is to investigate the axial stratification process and mechanism in the port injection SI engine. It is well known that the fuel is axially stratified in the combustion chamber through the combination of the injection timing and in-cylinder swirl motion and the final state of stratification governs engine stability and

lean misfire limit (LML) (Quader, 1981). There are many successful applications of this mechanism on the lean burn engine (Matsushita, 1985; Takeda, 1985; Horie, 1992; Harada, 1992; Nakanish, 1992; Ohm et al., 1993; Watanabe, 1993; Saito, 1994). However, the detailed mechanism of the stratification is not still fully disclosed.

In this paper, firstly the port swirl and tumble ratio were defined for classifying the port specifications and lean misfire limit of each ports were estimated as the function of the swirl ratio. After this definition, LML estimating was performed in various engines and swirl ratios with changing injection timing. In addition, gas fuel was used for eliminating the mixture preparation effect, i.e., evaporation of fuel on stratification. Lastly, air-fuel ratio (AFR) around the location of spark plug at ignition timing was investigated for confirming the effects of stratification due to swirl ratio and injection timing.

2. Experiments

2.1 Engine

A commercial 4-valve DOHC sequential MPI SI engine was modified as a single cylinder research engine. Four kinds of cylinder head of the same combustion chamber geometry have been used to induce in-cylinder flow of different swirl ratios. Another 3-valve SOHC multi-cylinder engines, which have different swirl ratios, were prepared for comparing DOHC. Specifications of the engine are given in Table 1.

The shapes of intake port of DOHC are shown in Fig. 1. Type-I port has the shape of original commercial DOHC engine and Type-II, III, and IV were modified ones to generate different swirl for this experiment. When the straight and swirl ports are open simultaneously (BPO : both ports open), no swirl is induced for Type-I. If the straight is closed and rear port (helical or straight) is open (RPO : rear port open), low swirl is generated. To get various swirl ratios, the cylinder head is replaced with the others. The port shapes of SOHC are not drawn because these are very

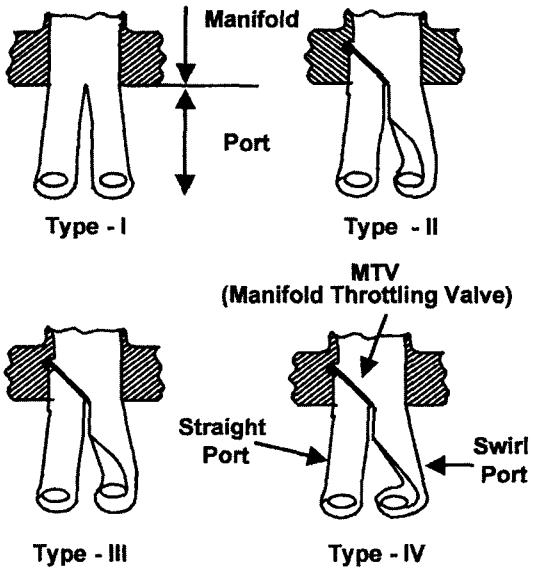

Fig. 1 Schematics of port (DOHC Engine)

Table 2 Test engine specifications

	DOHC	SOHC
No. Cylinder	1	4
No. of Intake Valve	2	2
No. of Exhaust Valve	2	1
Valve Timing (°CA)		
Intake Open	BTDC 5	BTDC 14
Intake Close	ABDC 35	ABDC 54
Exhaust Open	BBDC 35	BBDC 54
Exhaust Close	ATDC 5	ATDC 14
Combustion Chamber	Semi-Wedge	Pent Roof
Bore (mm)	75.5	←
Stroke (mm)	83.5	←
Max. Valve Lift (mm)	7.2	9

similar to that of DOHC. Five ports are prepared for the SOHC engine. In these ports, Type-III_S and Type-IV_S have the same shape and swirl ratio, but are symmetric to verify the effects of swirl direction. Therefore, the spark plugs are placed oppositely with respect to the swirl port in these two ports.

In the engine test, Lean Misfire Limit (LML) was evaluated with varying injection timing and swirl ratio. The LML was defined when misfire frequency is over 1% or brake mean effective pressure (BMEP) fluctuation is beyond 3%. The engine test condition was 1200rpm/1.5bar BMEP, 1500/1.5, 1800/2.0, 2000/2.0, 2200/2.5 and 2400/2.5.

2.2 Flow bench

The port characteristics are defined in a steady flow bench as Ricardo swirl number (RS) and tumble ratio. Moment of momentum flux was calculated from the angular velocity measured by Laser Doppler Anemometry (LDA). Figure 2 is a schematic of the steady flow bench for LDA measurement. A transparent quartz liner was used as a cylinder bore for optical measurement. Steady flow bench tests were made by varying valve lift from 1 mm to 8 mm by 1 mm increment. At each valve lift, the pressure drop across the port-valve assembly was maintained at 381 mm H_2O to keep the same velocity of intake air at valve opening area regardless of valve lift. All measurements were performed at 3×bore plane (250 mm apart from head) for full development of swirl and elimination of back flow effects in the cylinder. By measuring velocity components and flow rate in steady condition, the RS is calculated by the following equations (G. Cussion LTD, 1993; Heywood, 1988; Stone, 1992.):

$$R_s=\frac{\omega_s}{2\pi N}=\frac{\dfrac{BS}{\pi AD^2}\displaystyle\int_{\theta_1}^{\theta_2} C_f C_s d\theta}{\left(\displaystyle\int_{\theta_1}^{\theta_2} C_f d\theta\right)^2} \tag{1}$$

where,

$$C_s=\frac{8M}{\dot{m}v_0B},\quad C_f=\frac{4\dot{m}}{\rho v_0\pi D^2},\quad \omega_s=\frac{8}{B^2}\frac{\displaystyle\int_{\theta_1}^{\theta_2} Md\theta}{\displaystyle\int_{\theta_1}^{\theta_2}\dot{m}d\theta}$$

$$M=\int_0^{\frac{B}{2}}\int_0^{2\pi}\rho v_t(r,\theta)\,v_a(r,\theta)\,d\theta dr$$

The tumble ratio was also estimated with the same method as swirl measuring by adopting an L-shape tumble converter to the cylinder head.

2.3 High speed sampling

The high-speed gas sampling and analysis was used for measuring and tracing AFR at the spark plug in SOHC engines. The system consists of a Gas Chromatography (GC), a high speed gas sampling valve, a valve controller, a photo-electric pick-up, a vacuum pump and a high speed gas analyzer as shown in Fig. 3. The gas sampling line is connected to a 3-way valve to select GC or the gas analyzer. The high-speed gas sampling valve is needle-type, which is controlled by a valve controller to sample in-cylinder gas at any crank angle. The time delay of valve opening is one msec. The gas was sampled at the spark plug position only.

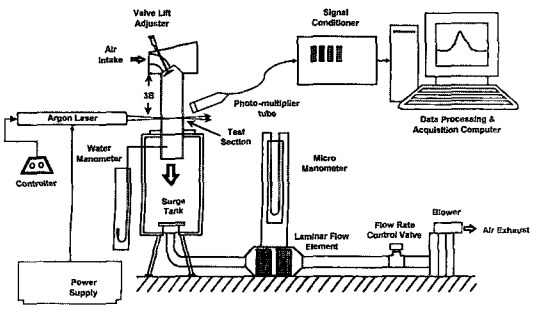

Fig. 2 Schematics of steady flow bench for LDV

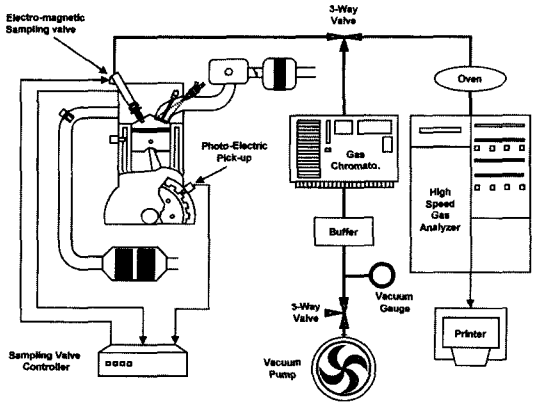

Fig. 3 Schematics of high-speed gas sampling and analyzing system

The AFR tracing was performed in intake and compression strokes. Before the sampling, the sampling line was made vacuous by the vacuum pump, and the sampling period was 15 CA (Crank Angle). The gas sampling was repeatedly continued until the pressure of sampling line reached atmospheric. In case of intake stroke, because the pressure of engine is too low to make sampled gas atmospheric, air was poured into the sampling line through the buffer line. The length of buffer line is 5 m, which is enough to prevent the mixing of the sampled gas and poured air. Condensation of the sampled gas was prevented by installing the tape type heater to the whole sampling line, and the temperature of the line was kept at 120 ℃. After this, the part of sampled gas, which was in sample loop of the GCs 6-port sampling valve, was sent to GC column and analyzed.

The GC used in the test is Varian 3400. The sampled gas was carried by 0.25 cc sample loop of the 6-port sampling valve. The capillary column is N 80/100 model of Porapak, which has 2 m length and 1/8″ diameter, stainless steel. The engine was motored at 1800 rpm and methanol was selected as the injected fuel because of its simplicity of the GC analysis.

The high-speed gas analyzer is also shown in Fig. 3. The test fuel was gasoline and sampling timing was firing BTDC 25 CA. The sampled gas was fed to gas analyzer by carrier gas(Helium) and analyzed.

The gas analyzer is Yanaco CGA-681H which can analyze 1～5 cc sampled gas within 6 sec. The analyzer consists of a TCD(Thermal Conductivity Detector) measuring sample gas volume, a Polargraph detector for O_2, two NDIRs for CO and CO_2, a FID for THC and CLD for NO.

3. Results and Discussion

3.1 Flow characteristics

Figure 4 shows the swirl and tumble ratio of

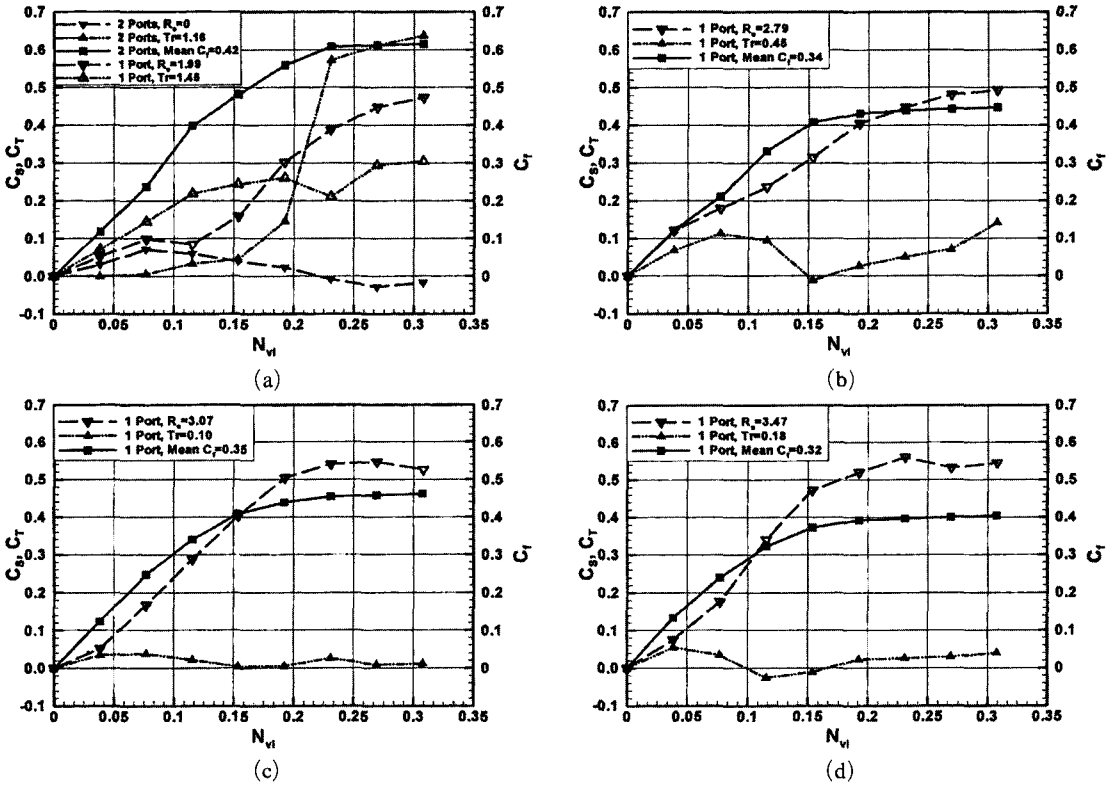

Fig. 4 Port characteristics of (a) Type-I (RS=0, 1.99), (b) Type-II (RS=2.79), (c) Type-III (RS=3.07) and (d) Type-IV (RS=3.47) as flow coefficient and swirl/tumble ratio

each port according to valve lift in DOHC engines. Non-Dimensional valve lift means the lift that is divided by valve inner sheet diameter. It can be seen that the order of tumble ratio is not negligible at low valve lifts compared with swirl regardless of swirl ratio except zero swirl case. In zero swirl case (BPO), both of swirl and tumble are very small at low valve lift. However, the tumble increases suddenly at high valve lift. In Table 2, port characteristics defined by RS, T_r and C_f are represented.

Figure 5 shows velocity fields of RS=0,1. 99, 2. 79 and 3.47 heads measured by LDV in the steady flow rig at 3×bore plane.

Almost zero swirl motion can be found when both of ports are open simultaneously and well developed swirl motion can be seen when only one is open. When swirl motion exists, each valve

Table 2 Port characteristics

DOHC				SOHC*		
RS	T_r	C_f		RS	C_f	
Type-I BPO	0	1.16	0.42	Type-I_S BPO	0	0.42
Type-I RPO	1.99	1.45	0.42	Type-I_S RPO	3.31	0.38
Type-II RPO	2.79	0.45	0.34	Type-II_S RPO	3.72	0.37
Type-III RPO	3.07	0.10	0.35	Type-III_S FPO	3.74	0.37
Type IV RPO	3.47	0.18	0.32	Type IV_S FPO	4.21	0.35

* RS are evaluated by impulse swirl meter

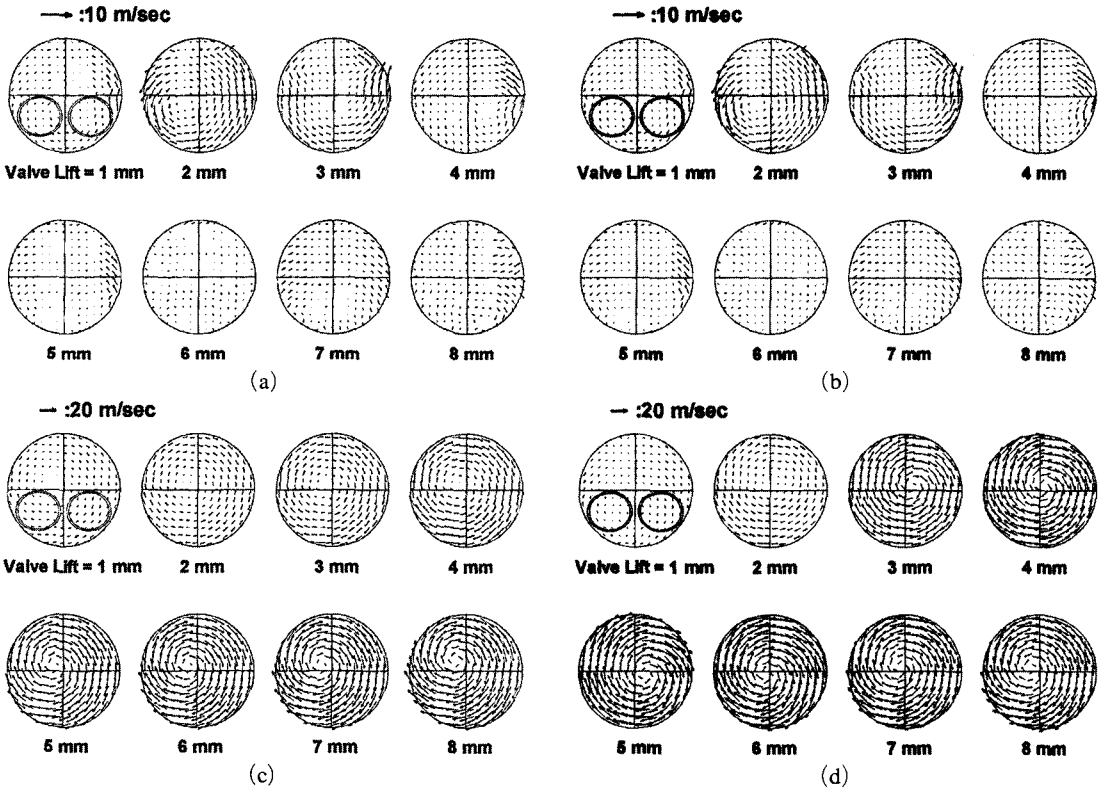

Fig. 5 Angular velocity profile at 3B position (a) Type-I (BPO, RS=0), (b) Type-I (RPO, RS=1.99), (c) Type-II (RPO, RS=2.79) and (d) Type-IV (RPO, RS=3.47)

lift can be classified as 3 typical regimes according to the velocity profiles. In the regime of low valve lift (valve lift 1, 2 mm), well-developed swirl motion cannot be seen. In the regime of medium valve lift (3, 4, 5 mm), swirl motion grows as valve lift increases. In the high valve lift (6, 7, 8 mm) regime, swirl motion is well developed and angular velocity is almost the same and saturated at each valve lift.

3.2 LML of engines

Figure 6 represents LML as a function of injection timing under no swirl condition in the DOHC engine (Type-I). The injection timing is defined as the end of injection signal. The effects of injection timing are observed only when fuel is injected during the intake process. On the contrary, LML remains constant when the fuel is injected during exhaust and compression strokes, allowing slightly different values according to engine speed.

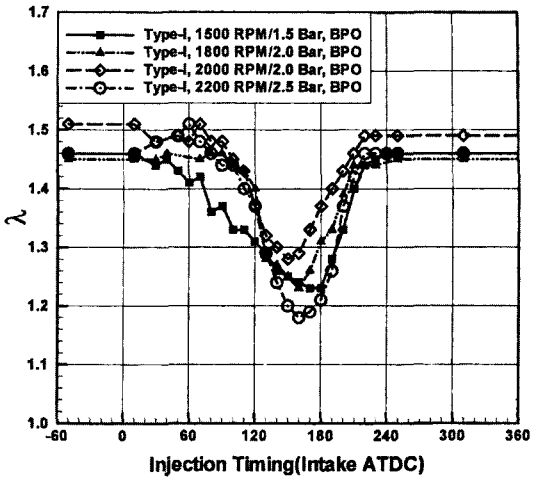

Fig. 6 LML as a function of injection timing in case of $RS=0$ (Type-I, BPO)

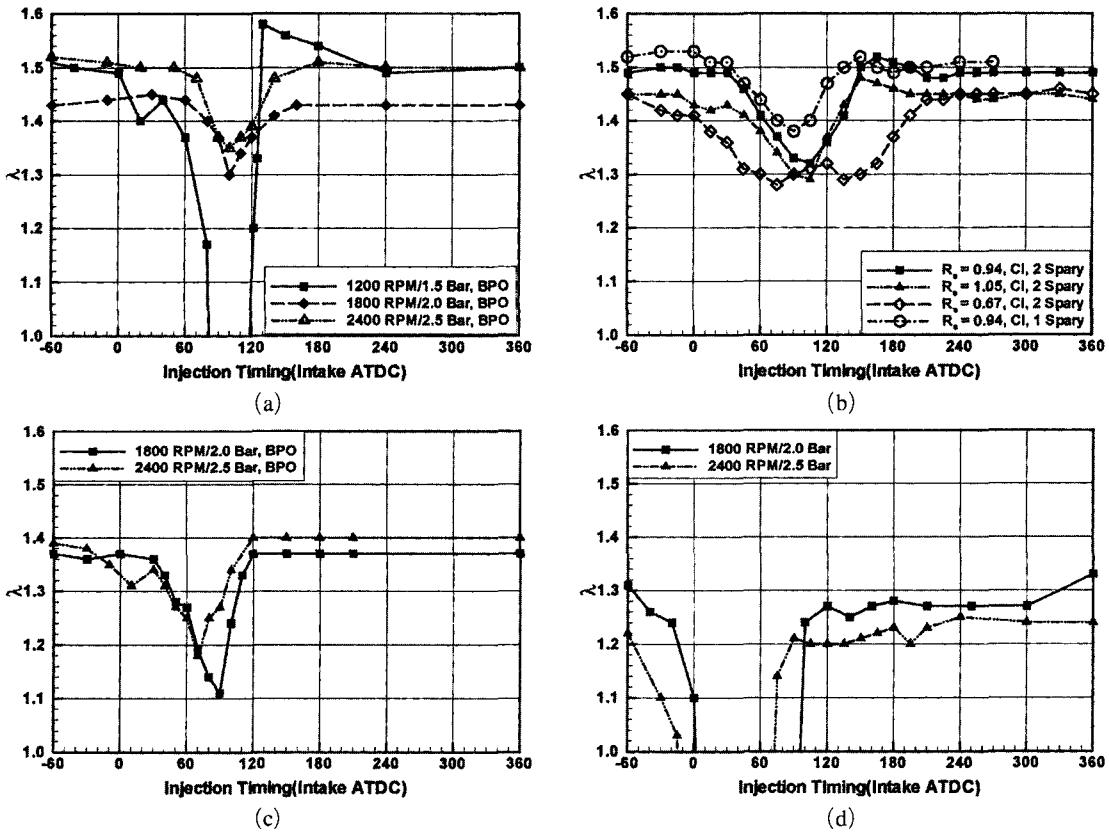

Fig. 7 LML as a function of injection timing in case of $RS=0$ and low swirl, (a) Type-I_S (BPO), (b) Type-I S (BPO+Port Masking), (c) 2.0L, 4 valve ($B=82$, $S=93.5$) and (d) 1.6L, 5 valve ($B=81$, $S=77$)

When no swirl is induced (BPO), LML decreases down to 1.2~1.3 around at 150 CA and start to recover to each constant LML value specified by the engine speed. In the multi-intake valve system, the swirl motion is hardly formed because of two or three parallel flow components. Figure 7 represents the LML investigation results through various multi-intake valve engines. As shown in the figure, there is no exception in the fact that the intake stroke injection induces very low LML under zero or very low swirl in case of multi-intake ports. The swirl ratio of engine in Fig. 7(b) is controlled by inserting a plate into upstream of Type-I_S engine port.

All LML results of DOHC engines are shown in Fig. 8 as a function of the injection timing when the swirling motion exists (RPO). In these cases, the intake stroke injection expands LML considerably. LML increases up to the highest AFR of 1.55, 1.69, 1.70 and 1.75 at around 150 CA for RS=1.99, 2.79, 3.07 and 3.47, respectively. It is also observed that the highest attainable LML increases as RS increases in DOHC engines. In addition, the injection timing for the highest attainable LML slightly advances as RS increases. Figure 9 is the results of SOHC engine operation. In general, there is no difference in the tendency of LML as a function of swirl ratio and injection timing between DOHC and SOHC. However, the optimum timings are advanced and slightly higher LML is observed in SOHC. In addition, there exists an optimum swirl ratio in SOHC engines. It is supposed that increasing of port wall wetting restrains LML expansion in extremely high swirl (Fig. 9(d), RS=4.21).

In Fig. 10, LML investigation results of two commercial lean burn engines are represented. As shown in the figure, the fact that the intake

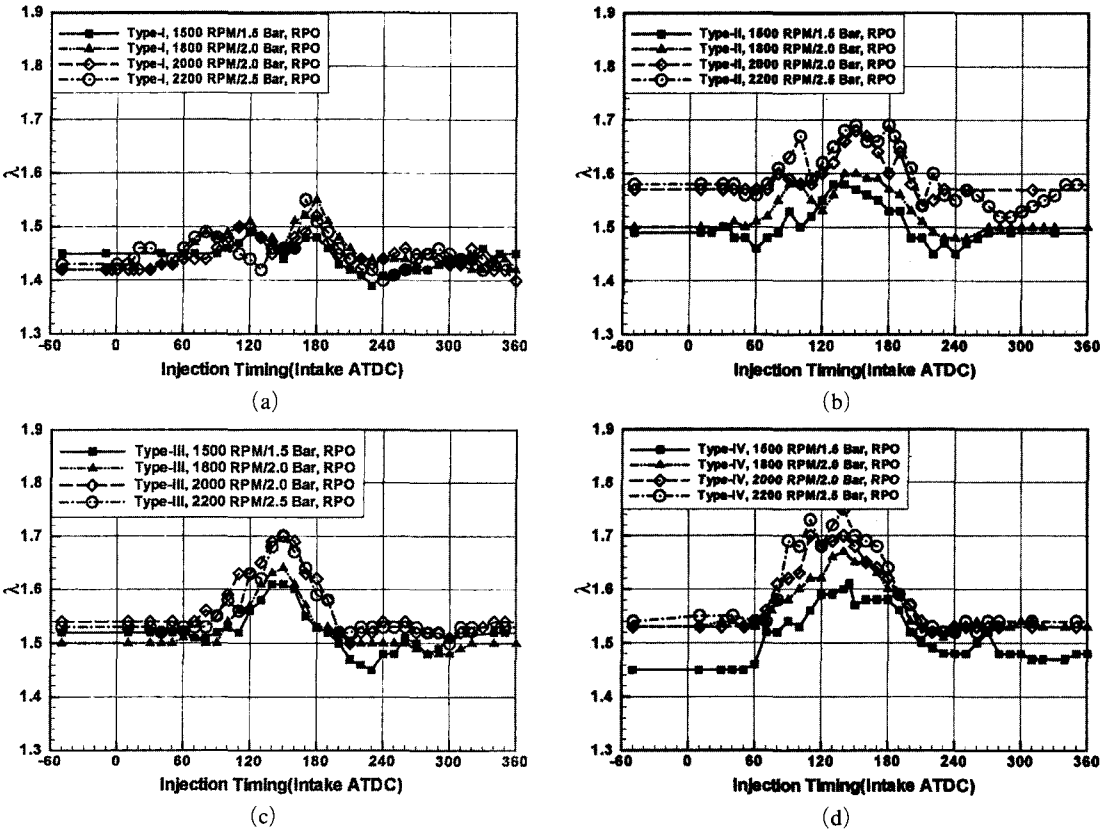

Fig. 8 LML as a function of injection timing and swirl ratio, (a) Type-I (RPO, RS=1.99), (b) Type-II (RPO, RS=2.79), (c) Type-III (RPO, RS=3.07) and (d) Type-IV (RPO, RS=3.47)

stroke injection improves LML under the high swirl condition is not changed. However, the LML curves have slightly different shapes. The band of LML expanding zone is wider than that of the previous case and optimum timings are advanced at about 60~90 CA.

After observing all LML results in various engines and swirl ratios, it can be concluded that

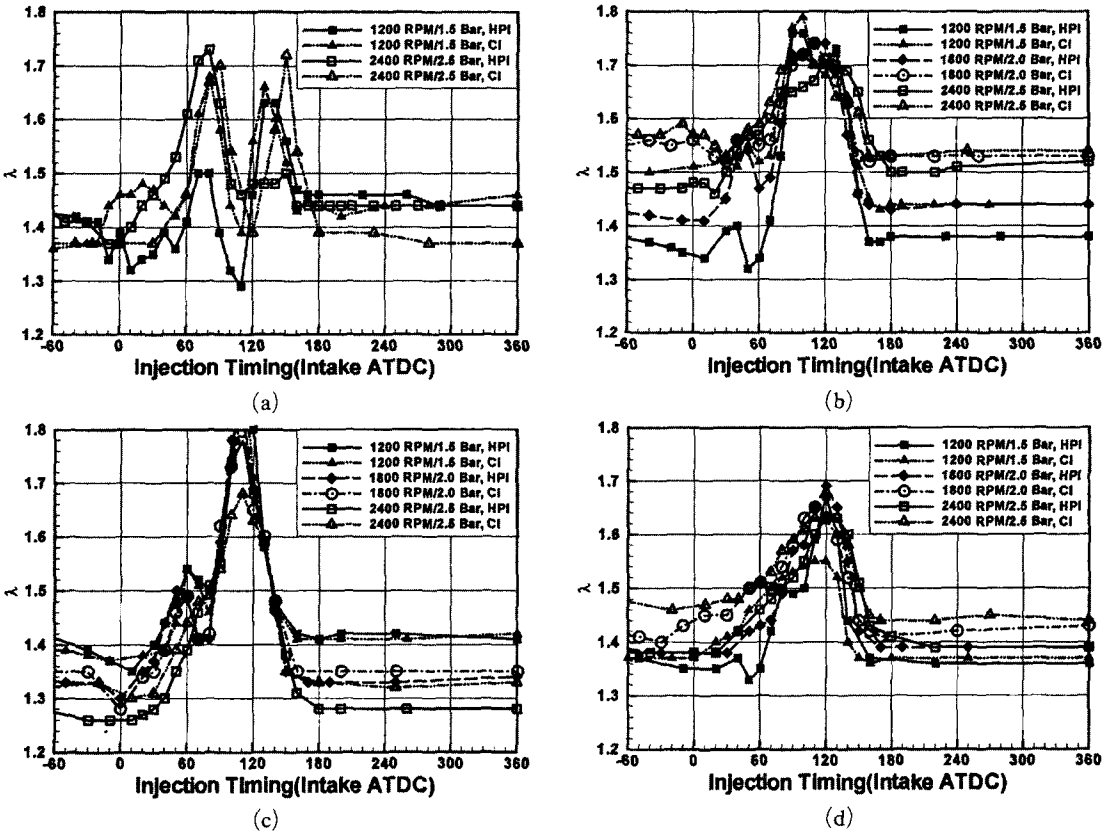

Fig. 9 LML as a function of injection timing and swirl ratio, (a) Type-II_S (RPO, RS=3.31), (b) Type-III_S (RPO, RS=3.72), (c) Type-IV_S (FPO, RS=3.71) and (d) Type-V (FPO, RS=4.21)

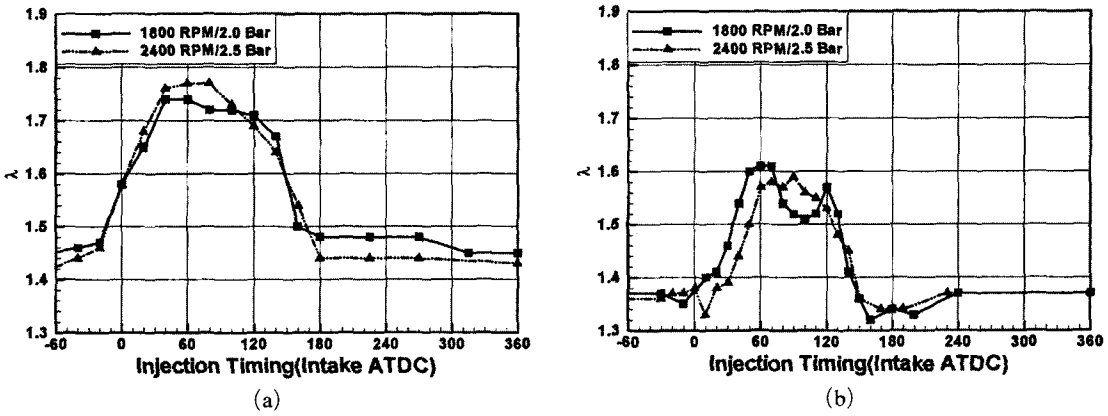

Fig. 10 LML as a function of injection timing and swirl ratio, (a) 1.6L, 4 valve (FPO, B=81, S=77, RS=3.66), (b) 1.5L, 4 valve (RPO, B=75.0, S=84.5, RS=4.25)

the intake stroke injection highly affects LML without exception. Because the intake stroke duration, i.e., air induction duration, is much more longer than that of fuel injection, complete mixing of air and fuel might be impossible in the cylinder at the part load condition. Therefore, non-uniformity of mixture distribution, so called stratification, always takes place. It can also be said that the charging state is heterogeneous though injection timing is not in intake stroke (late injection), since the late injected fuel enters the cylinder at once during the early intake stage. This means the stratification always take places in all fuel injection systems. This stratification was reported even in a single point injection (SPI) engine (Takeda, 1985). However, the optimum/worst injection timings and highest/lowest LML have different values according to the port characteristics, swirl generation mechanism and injection characteristics.

On the other hands, it is obvious that favorable mixture distribution to high LML is the one in which rich mixture is formed near an ignition point. The stable and strong initial flame due to the rich mixture ensures high LML and reduces cyclic variation. Though the relative positions of spark plug and helical ports are horizontally opposite in RPO and FPO case, there is no difference in LML as a function of injection timing in SOHC as shown in the Figs. 9(b) and 9(c). In this context, the stratification by swirl and injection timing is deduced as axial distribution.

A particular phenomenon is observed at a singular swirl ratio. As shown in Figs. 7(a) and 8(a), bi-modal LML patterns appear when the swirl ratio is not sufficient as 1.99 in DOHC and 3.31 in SOHC. Considering the change of swirl ratio from 3.72 to 3.3 and from 2.79 to 1.99 is not large, this transition is very remarkable. This bi-modal phenomenon is more clearly observed in SOHC engines. Moreover, in high swirl port, weak first LML peak is formed before optimum injection timing (Figs. 7(b), 8(b) and (8c)).

It means the process of axial stratification is not a simple mechanism. It is supposed that at least two different processes are mixed in the complete axial stratification mechanism. It is also supposed that the predominant process is changed as the swirl ratio and injection timing are varied. In these processes, two-phase flow effect including evaporation of the injected fuel and complicated in-cylinder air motion might play a certain role.

3.3 AFR at spark plug

Prior to examination of the stratification process, local AFR formation was investigated by high-speed gas sampling for understanding the stratification process qualitatively.

Figure 11 is the results of AFR measurement at the spark plug location by high-speed sampling and analysis and that of LML, which is investigated in the same engine and operating condition. A Type-V_S engine was used for the measurement and total exhaust AFR was kept as stoichiometric. As shown in the figure, the AFR at the spark plug and LML are very closely related. In case of no swirl, AFR at the spark plug becomes much leaner than that of exhaust by the intake stroke injection. The leanest AFR is about 1.3 at 120 CA. In the other strokes, the AFR remains around stoichiometric. Therefore the intake stroke injection forms lean mixture at the spark plug, which results in low LML. On the contrary, rich mixture is formed at the spark plug by the intake stroke injection in the high swirl case. The timing when the richest mixture is formed coincides with that of the highest LML (Figs. 11(c) and 11(d)). This means that the stratification affects LML through AFR preparation at the spark plug.

On the other hand, the in-cylinder fuel motion during intake and compression strokes is affected by the in-cylinder flow motion. In addition, the flow patterns have different characteristics as the cycle porceeds because of the changing of intake valve lift and piston position. Therefore, the fuel motion injected in the cylinder must be varied, if the fuel injection timing were varied. For understanding the process of mixture formation at the spark plug, the injected fuel behavior was tracked by high-speed sampling during the intake and compression stroke. If the injected fuel were detected at a specified position, the bulk air

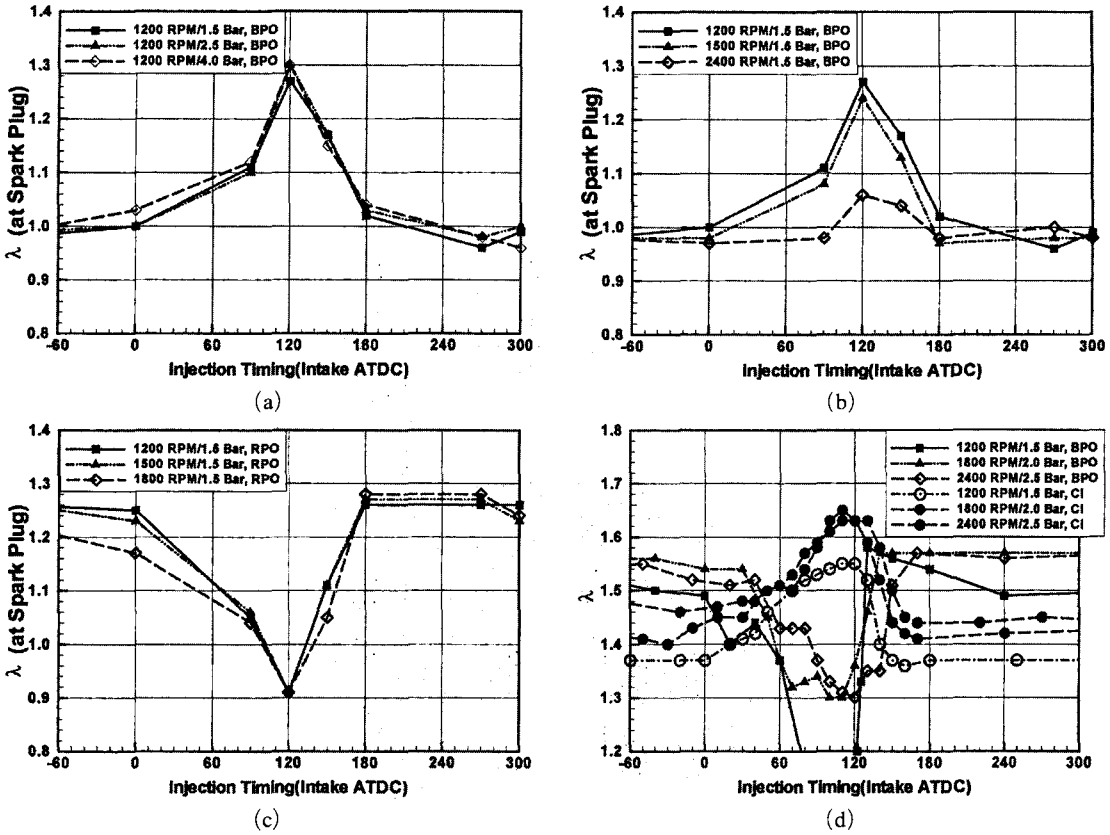

Fig. 11 Relationship between AFR at spark plug and LML (Type-V_S) at (a) 1200 RPM, BPO, (b) 1.5 Bar BMEP, BPO, (c) 1.5 Bar BMEP, FPO and (d) LML at corresponding condition

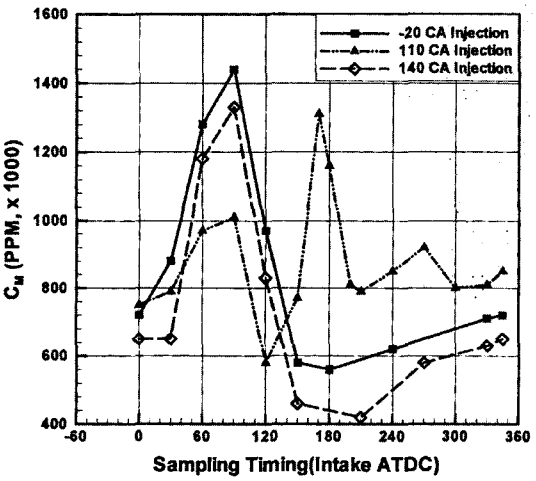

Fig. 12 Variation of fuel concentration at spark plug during intake and compression stroke

motion in the cylinder and the effect of the injection timing on LML could be deduced.

Figure 12 shows methanol concentration, which is sampled at spark plug and analyzed by GC after small amount of methanol is injected in the cylinder. In case of BTDC 20 CA injection, the detected methanol has the maximum value when it is not sampled at early intake stroke but sampled at ATDC 90 CA. Subsequently, the detected quantity is decreased to have the minimum value at about BDC and increased slightly again as a piston goes up.

In case of ATDC 110 CA, which is the injection timing of the highest LML, the detected quantity has the maximum value when sampled at 170 CA. Therefore, it is considered that it takes about 60 CA for the injected fuel to come into the cylinder and reach at the spark plug. This means that the fuel injected at optimum injection timing comes into the cylinder at the end stage of intake because the real intake motion is finished near

BDC. The fuel injected at ATDC 110 CA is also considered to be strongly stratified and to pass through spark plug at very high speed and then remain stratified until later compression stroke because the maximum peak width is very narrow and the detected quantity goes up and down during the compression stroke. It is considered that the oscillation of fuel in compression stroke is caused by the strengthened swirl motion.

In case of 140 CA, the fuel quantity curve is the same as the injection timing BTDC 20 CA. Therefore it is supposed that most fuel injected ATDC 140 CA cannot come into the cylinder in this cycle because of low air velocity and back flow, and that it comes into the cylinder in the next cycle while the intake valve is being opened.

As a result, the variation of injection timing results in the variation of the fuel quantity sampled at spark plug position. In addition, the richest mixture formed at the spark plug when the injection is performed in the optimum injection timing. Until now, however, it is not possible to describe the LML bi-modal phenomenon based on only this high-speed sampling. Because the point measure provides spatially limited information, it is impossible to grasp detailed process of stratification through the high-speed sampling. Though the high-speed sampling shows that AFR at the spark plug is rich in the optimum injection timing, it cannot give any information about how and from where the fuel comes to the spark plug.

3.4 Gas fueling

Because the gasoline is liquid fuel, it has to evaporate in the port and cylinder. If the fuel evaporation amount is not negligible during the intake and compression stroke, it might affect the process. For confirming the effects, compressed natural gas (CNG) was used as fuel in engine test for engine speed 1500 and 1800 RPM and the results are shown in Fig. 13. The injector has been specially designed for CNG fueling.

As shown in Fig. 13(a), the intake stroke injection lowers LML as like as the gasoline fueling. If the evaporation effect of fuel is not negligible, then this may be most distinct in BPO because the air induction speed is relatively low and the time for the evaporation is short compared with one port deactivation. The fact that the intake stroke injection of gas fuel also lowers LML might suggest that the stratification is not much affected by the fuel evaporation. In all swirl ratios, the patterns of LML are not significantly affected by fuel phase (i.e., gaseous or liquid) but by injection timing and swirl ratio. The optimum injection timing of CNG fueling is retarded at about 40 CA compared with the gasoline fueling. It is supposed that faster penetration velocity of gas fuel causes this timing difference. Because the CNG fuel arriving time at valve is faster than that of gasoline at about 40 CA at 1500 RPM (Ohm, 1997), the 40 CA retarded injection timing of CNG means almost the same arrival timing at valve as gasoline.

Throughout all LML investigation, it is found that the LML as a function of injection timings are almost the same for a given swirl ratio regardless of engine speed and no considerable LML variation according to the engine speed was observed. In general, the engine speed is directly related to intake air velocity and accordingly the turbulence intensity at the final stage of compression. It is well known that intensified turbulence by increased engine speed promotes combustion so that the mixture in combustion chamber can be burnt during almost the same crank angle regardless of engine speed. Therefore, the faster combustion due to increased turbulence becomes possible at higher engine speed. However, the observation that LML is not significantly affected by engine speed suggests that the high LML is obtained not by turbulence but by AFR around the spark plug at the ignition timing.

It means that the early flame stability and intensity due to stratification, which are supposedly governed by in-cylinder bulk air motion, are much more important factor to expand LML and ensure overall engine stability than the fast burn induced by turbulence increase due to high intake air velocity which can be achieved, for example, through high engine speed (Stone, 1992; Kalghatgi, 1987).

Therefore it can be said that LML or stability

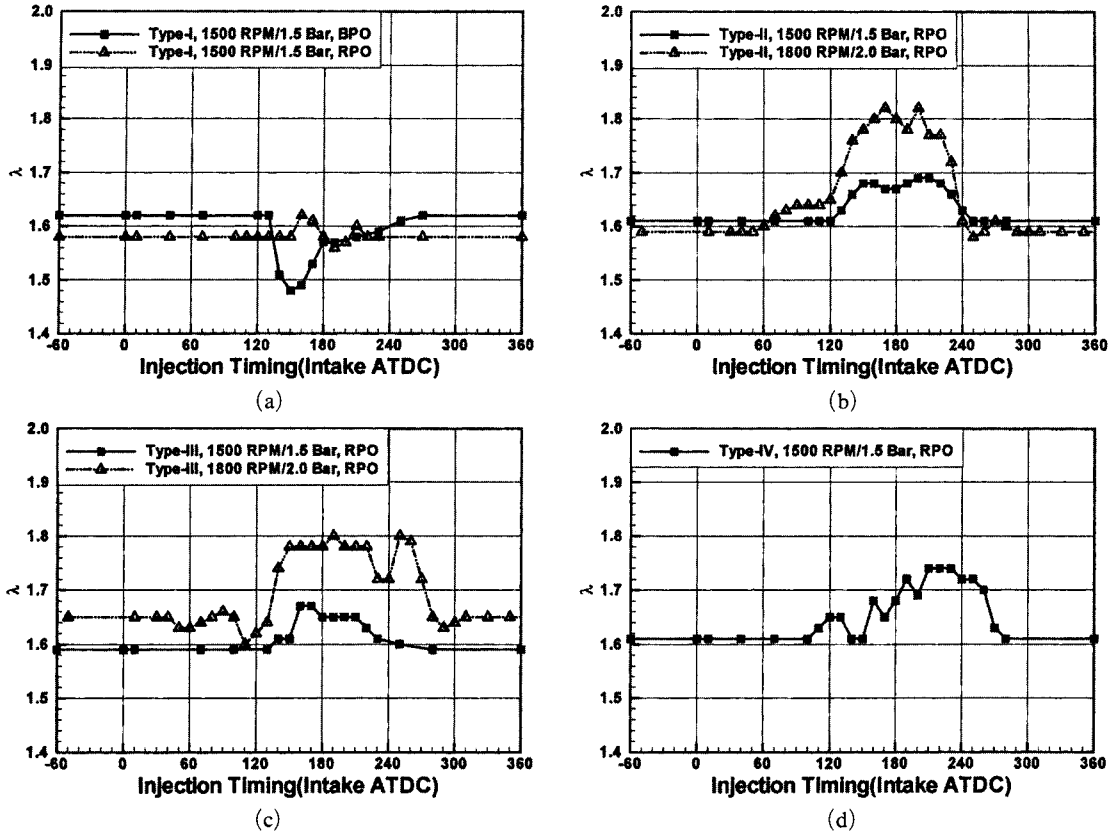

Fig. 13 LML of CNG fueling, (a) Type-I (BPO, RS=0 and RPO, RS=1.99), (b) Type-II (RPO, RS=2.79), (c) Type-III (RPO, RS=3.07) and (d) Type-IV (RPO, RS=3.47)

of engine is rather governed by macroscopic factors such as swirl ratio and combined effect of swirl and injection timing, i.e. stratification than by microscopic phenomena such as turbulence or mean absolute velocity of intake air.

From the all engine test observations, it is believed that mainly the bulk air motion in the cylinder governs the fuel stratification and the effect of vaporization and fuel droplets is relatively weak. Therefore, it is necessary to understand the fuel stratification mechanism through in-cylinder air motion and trajectory of the injected fuel, i.e., time and spatial history of the flow and fuel. In other words, it is very important for understanding stratification to know in which part of induction air the fuel exists, how and where this fuel moves in the cylinder as affected by air motion and how the final fuel distribution state is at the spark event in the combustion chamber according to the injection timing and swirl ratio.

4. Conclusions

Through the port evaluation on steady flow bench, LML measurement of engines and AFR measurement at the spark plug positions, the following conclusions are drawn :

(1) The order of tumble ratio is not negligible at low valve lifts compared with swirl, regardless of swirl ratio except zero swirl case. In zero swirl case, both of swirl and tumble are very small at the low valve lifts. However, the tumble increase suddenly at the high valve lifts.

(2) When swirl motion exists, well-developed swirl motion cannot be seen in the low valve lift region. The swirl motion grows as valve lift increases in the medium valve lift region and

finally the angular velocity is almost saturated in the high valve lift region.

(3) Stratification phenomenon is always observed when fuel is injected in the intake stroke regardless of swirl ratio and fuel state.

(4) Air-fuel ratio at the spark plug is heavily related to the rig swirl ratio and the injection timing. Intake stroke injection induces rich-mixture formation under the high swirl condition and lean-mixture formation under the low or no swirl condition.

(5) The governing parameter of lean misfire limit is Air-fuel ratio around the spark plug, which is a result of stratification. Rich-mixture formation around the spark plug due to suitable combination of the injection timing and swirl flow achieves high lean misfire limit.

(6) Evaporation of fuel does not affect the stratification mechanism. The stratification phenomenon is mainly governed by bulk air motion in the cylinder.

(7) The single point measurement of fuel concentration does not offer sufficient information about the stratification phenomenon. For thorough understanding of stratification, it is necessary to grasp time and spatial history of fuel behavior in the cylinder.

Acknowledgment

This work was supported by the research fund of Seoul National University of Technology.

References

Cussion, G., LTD, 1993, *Flow bench Super-Flow 600 Manual*.

Harada, J., 1992, "Development of a New Generation Lean Burn Engine," SAE Paper 920468.

Heywood J. B., 1988, *Internal Combustion Engine Fundamentals*, McGraw-Hill, Singapore, pp. 343～345.

Horie, K., 1992, "The Development of High Fuel Economy and High Performance Four-Valve Lean Burn Engine," SAE Paper 920455.

Kalghatgi G. T., 1987, "Spark Ignition, Early Flame Development and Cyclic Variation in IC Engines," SAE Paper 870163.

Matsushita, S., 1985, "Development of the Toyota Lean Combustion System," SAE Paper 850044.

Matsusita, S., 1985, "Effects of Helical Port with Swirl Control Valve on the Combustion and Performance of SI Engine," SAE Paper 850046.

Nakanish K., 1992, "Development of a new intake system for a 4-valve lean burn engine," SAE Paper 920520.

Ohm I. Y., Ahn H. S., Lee W. J., Kim W. T., Park S. S. and Lee D. U., 1993, "Development of HMC Axially Stratified Lean Combustion Engine," SAE Paper 930879, SAE Transaction 103 Vol. 3, pp 1298～1311.

Ohm I. Y., Jeong K. S. and. Jeung I. S, 1997, "Effects of Injection Timing on the Lean Misfire Limit in an SI Engine," SAE Paper 970028, SAE Transactions 106, Vol. 3, pp. 42～55.

Quader, A. A., 1982, "The Axially-Stratified-Charge Engine," SAE Paper 820131.

Saito F., 1994, "Mazda Advanced Lean Burn Engine with New Three-Way Catalyst," SAE Paper 940506.

Stone R., 1992, *Introduction to Internal Combustion Engine*, MACMILLAN, London, pp. 183～185.

Stone R., 1992, *Introduction to Internal Combustion Engine*, MACMILLAN, London, pp. 140～143.

Takeda, K., 1985, "Toyota Central Injection (CI) System for Lean Combustion and High Transient Response," SAE Paper 851675.

Watanabe T., 1993, "Optimization of In-Cylinder Flow and Mixing for the Center Spark Four Valve Lean Burn Engine Employing the Concept of Barrel-Stratification," SAE Paper 930585.